Cancer Letters 339 (2013) 15–24

Contents lists available at ScienceDirect

Cancer Letters

journal homepage: www.elsevier.com/locate/canlet

Depletion of end-binding protein 1 (EB1) promotes apoptosis of human non-small-cell lung cancer cells via reactive oxygen species and Bax-mediated mitochondrial dysfunction

Min-Jung Kim [a,1], Hong Shik Yun [a,b,1], Eun-Hee Hong [a,b], Su-Jae Lee [b], Jeong-Hwa Baek [a,c], Chang-Woo Lee [c], Ji-Hye Yim [a], Jae-Sung Kim [a], Jong Kuk Park [a], Hong-Duck Um [a], Sang-Gu Hwang [a,*]

[a] Division of Radiation Cancer Biology, Korea Institute of Radiological and Medical Sciences, Seoul 139-706, Republic of Korea
[b] Department of Chemistry, College of Natural Sciences, Hanyang University, Seoul 133-791, Republic of Korea
[c] Department of Molecular Cell Biology, Samsung Biomedical Research Institute, Sungkyunkwan University School of Medicine, Suwon, Gyeonggi 440-746, Republic of Korea

ARTICLE INFO

Article history:
Received 25 April 2013
Received in revised form 15 July 2013
Accepted 24 July 2013

Keywords:
EB1
Apoptosis
Radiation
Mitochondrial ROS
Bax

ABSTRACT

Although end-binding protein 1 (EB1) is well known to regulate microtubule dynamics, the role of EB1 in apoptosis of non-small cell lung cancer (NSCLC) is poorly understood. Here, we investigated the molecular mechanism by which EB1 regulates apoptosis in H460, A549, and H1299 cells. Depletion of EB1 in A549 and H1299 cells, which express high levels of EB1, induced cell death in a p53-independent manner through over-production of reactive oxygen species (ROS) and Bax induction. This phenomenon was potentiated in radiation-treated EB1-knockdown cells and was largely blocked by N-acetyl-L-cysteine, a scavenger of ROS. ROS accelerated the activation of nuclear factor-kappa B (NF-κB) to promote transcriptional activity of Bax, an action that was accompanied by cytochrome c translocation and apoptosis-inducing factor (AIF) release. The NF-κB inhibitor, BAY 11-7082, potently inhibited the apoptosis induced by EB1 knockdown and radiation treatment, in association with diminished activity of the mitochondrial death pathway. Conversely, ectopic overexpression of EB1 in H460 cells, which express low levels of EB1, remarkably abrogated radiation-induced apoptosis and NF-κB-mediated mitochondrial dysfunction. Our data provide the first demonstration that down-regulation of EB1 promotes NSCLC cell death by inducing ROS-mediated, NF-κB-dependent Bax signaling cascades, a process in which cytochrome c and AIF play important roles, indicating a potential therapeutic benefit of EB1 in lung cancer.

1. Introduction

When a lung tumor cannot be removed by surgery because of its size or location, radiation therapy (often in combination with chemotherapy) may be used as the main treatment. Despite the effectiveness of radiotherapy in cancer treatment, lung tumor cells may repopulate the primary tumor or metastatic sites, an outcome largely attributable to radioresistance [1,2]. Non-small-cell lung cancer (NSCLC) represents a heterogeneous group of lung cancers that can occur as unusual histologic variants and thus are relatively insensitive to radiotherapy compared with small-cell lung cancer and other cancers [3,4]. Therefore, new strategies, such as biomarker-integrated targeted therapeutic approaches, are needed to achieve improved survival in patients with locally advanced, unresectable disease or advanced metastatic disease.

Mitochondria, the energy factories of the cell, play a key role in the regulation of cell death as well as signaling and cellular differentiation [5]. Mitochondrial molecules involved in reactive oxygen species (ROS) generation, Bcl-2 down-regulation, Bax activation, cytochrome c release, apoptosis inducing factor (AIF) release, and caspase-3 activation have been reported to regulate apoptosis in various cell lines [6,7]. It has been shown that the mitochondrial membrane permeabilization pore is sensitive to the redox state, and ROS can facilitate mitochondrial membrane permeabilization both *in vitro* and *in vivo* [8]. Dysregulation of the levels of Bax and Bcl-2 disrupts mitochondrial function, causing the release of

Abbreviations: AIF, apoptosis inducing factor; EB1, end-binding protein 1; NAC, N-acetyl cysteine; NSCLC, non-small-cell lung cancer; NF-κB, nuclear factor-kappa B; PARP, poly (ADP-ribose) polymerase; ROS, reactive oxygen species; siRNA, small interfering RNA.

* Corresponding author. Address: Division of Radiation Cancer Biology, Korea Institute of Radiological and Medical Sciences, 75 No-won gil, No-won Gu, Seoul 139-706, Republic of Korea. Tel.: +82 2 970 1353; fax: +82 2 970 2417.
E-mail address: sgh63@kcch.re.kr (S.-G. Hwang).
[1] These authors contributed equally to this work.

0304-3835
http://dx.doi.org/10.1016/j.canlet.2013.07.027

cytochrome c from mitochondria into the cytosol and subsequent activation of caspase cascades, the terminal step in the apoptotic process [9,10]. Bax, a pro-apoptotic protein of the Bcl-2 family, mainly resides in the cytosol of healthy cells; however, following initiation of death signaling, it integrates and oligomerizes into the outer mitochondrial membrane (OMM). These oligomers are thought to induce permeabilization of the OMM, allowing the efflux of apoptogenic proteins [11,12].

Human end-binding protein 1 (EB1) was originally identified as an interacting partner of adenomatous polyposis coli (APC) that acts to enhance APC function in colorectal cancer [13]. EB1, a member of the plus-end-tracking protein family, acts as not only a microtubule-stabilization factor but also as an anti-pausing factor, promoting microtubule dynamics [14–16]. Recent studies suggest that EB1 is associated with a variety of microtubule-mediated cellular activities in various systems, including migration, cell division, and morphogenesis [17–20]. Notably, EB1 has been reported to be overexpressed in gastric adenocarcinoma [21], hepatocellular carcinoma [22], esophageal squamous cell carcinoma [23], and breast cancers [24]. This up-regulation might be involved in tumorigenesis and promotion of tumor cell growth via the Wnt signaling pathway or Aurora-B activation [23–25]. However, the molecular role of EB1 in regulating tumor cell death, especially in the context of lung cancer cells radioresistance, remains to be elucidated.

In this study, we investigated the cytotoxicity of EB1 in NSCLC cells and found that depletion of EB1 promoted apoptotic cell death via mitochondrial ROS production. We further explored the EB1 signaling mechanism to determine the downstream effectors of accumulated ROS in radiation-treated lung cancer cells.

2. Materials and methods

2.1. Cell culture and treatment

BEAS-2B human normal bronchial cells, SiHa human cervical cancer cells, MCF-7 human breast cancer cells, and H460, A549 and H1299 human NSCLC cells were purchased from American Type Culture Collection (Manassas, VA, USA). HCT116 $p53^{+/+}$ and $p53^{-/-}$ isogenic human colon cancer cell lines were kindly provided by Professor Bert Vogelstein (The Johns Hopkins University, Baltimore, MD, USA). BEAS-2B, H460, A549, and H1299 cells were grown in Roswell Park Memorial Institute (RPMI)-1640 medium. SiHa, MCF-7, HCT116 $p53^{+/+}$, and HCT116 $p53^{-/-}$ cells were maintained in Dulbecco's modified Eagle's medium. Cells were incubated at 37 °C in a humidified incubator with 5% CO_2, and medium was supplemented with 10% fetal bovine serum, 50 μg/mL streptomycin, and 50 units/mL penicillin. The cells were irradiated using a ^{137}cesium-ray source (Atomic Energy of Canada Ltd., Mississauga, Canada) at a dose rate of 3.81 Gy/min. Where indicated, cells were treated with 1 mM N-acetyl cysteine (NAC; Sigma, St. Louis, MO, USA) to scavenge ROS or 1 μM BAY 11-7082 (BAY; Calbiochem, San Diego, CA, USA) to inhibit NF-κB activity.

2.2. Cell proliferation

Cells were plated on culture dishes at a density of 5×10^4 cells/cm^2 for the indicated times with or without small interfering RNA (siRNA)-mediated EB1 knockdown. Cell proliferation was determined by direct counting using a hemocytometer.

2.3. Assay for cell death

Cells seeded at a density of 2×10^5 cells per 60-mm dish were left untreated or were treated with 10 Gy radiation under the indicated experimental conditions. For quantification of cell death, cells were trypsinized, washed in phosphate-buffered saline (PBS), dually stained with annexin V and propidium iodide, and analyzed with a FACScan flow cytometer (Becton Dickson, Franklin Lakes, NJ, USA). Apoptotic cell death was also determined by Western blot analysis of cleaved poly (ADP-ribose) polymerase (PARP) and activated caspase-3. Alterations in cellular morphology were observed by light microscopy.

2.4. Colony-forming assay

Cell survival before and after irradiation was determined using clonogenic assays, as described previously [26]. Cells were left untreated or were treated with a single dose of radiation ranging from 0 to 5 Gy, according to the indicated experimental conditions, and then were trypsinized, diluted, and seeded into 60-mm tissue culture dishes. After 14 days, colonies were fixed with methanol and stained with trypan blue solution. Colonies with 50 or more cells were counted as survivors using a colony counter (Imaging Products, Chantilly, VA, USA).

2.5. Immunofluorescence confocal microscopy

H460 and A549 cells were fixed with 3.5% paraformaldehyde in PBS, as described previously [27]. Cells were permeabilized by incubating for 30 min with PBS containing 0.1% Triton X-100 and blocked by incubating with PBS/5% fetal bovine serum for 30 min. Cells were washed with PBS and incubated with 10 μg/mL of mouse monoclonal anti-EB1 primary antibody (Santa Cruz Biotechnology. Inc., Santa Cruz, CA, USA) for 1 h. The cells were incubated with fluorescein isothiocyanate (FITC)-conjugated secondary antibody (Invitrogen, Carlsbad, CA, USA) and then observed with a laser-scanning confocal microscope (Leica Microsystems, Heidelberg, Germany). Cell nuclei were identified by staining with 4,6-diamidino-2-phenylindole (DAPI).

2.6. ROS assay

H460 and A549 cells were left untreated or were treated with 10 Gy radiation in the absence or presence of NF-κB inhibitor, as indicated. Cells were incubated with 10 nM 2′,7′-dichlorofluorescein diacetate (DCF-DA; Molecular Probes. Inc., Eugene, OR, USA) to detect ROS, as described previously [28]. Cells were initially harvested by trypsinization and then analyzed for DCF-DA fluorescence using a FACScan flow cytometer. ROS levels were expressed as a histogram of the fluorescence generated by 10,000 cells. Cell staining was subsequently examined with a laser-scanning confocal microscope (Leica Microsystems) using on an excitation wavelength of 488 nm and a 525-nm emission filter. Mitochondrial superoxide generation was detected by staining cells for 10 min at 37 °C with 5 μM MitoSOX Red, a mitochondrial superoxide indicator for live-cell imaging (Invitrogen), and then washing three times with PBS before imaging. Groups of cells were randomly selected from each sample.

2.7. Reverse transcription-polymerase chain reaction (RT-PCR)

Total RNA was isolated using RNA STAT-60 (Tel-Test B, Inc., Friendswood, TX, USA). RT reactions were performed using ImProm-II reverse transcriptase (Promega, Madison, WI, USA) with r*Taq* polymerase (iNtRON, Gyeonggi-do, Korea) by incubating for 5 min at 70 °C (annealing) and 60 min at 42 °C (first strand extension). The following conditions and primer pairs were employed for conventional PCR: EB1 (333 bp product; annealing temperature, 57 °C; 28 cycles), 5′-CTG CGT ATT GTC AGT TTA TG-3′ (sense) and 5′-GAG GTT TCT TCG GTT TAT TC-3′ (antisense); glyceraldehyde-3-phosphate dehydrogenase (GAPDH) (305 bp product; annealing temperature, 55 °C; 24 cycles), 5′-CAT CTC TGC CCC CTC TGC TGA-3′ (sense) and 5′-GGA TGA CCT TGC CCA CAG CCT-3′ (antisense). The amplification signals of the target gene were normalized against that of GAPDH in the same reaction.

2.8. Knockdown of EB1 by siRNA

The following EB1-specific siRNA based on the sequence of human EB1 was synthesized according to the manufacturer's guidelines (Genolution, Seoul, Korea): 5′-UUG CCU UGA AGA AAG UGA AUU-3′ (sense) and 5′-UUC ACU UUC UUC AAG GCA AUU-‘3 (antisense). A scrambled siRNA, which showed no significant homology to known gene sequences and did not regulate gene expression, was used as a negative control. Cells were transfected with 100 nM siRNA in serum-free medium for 5 h using Metafectene reagent (Biontex, München, Germany) according to the manufacturer's protocol, as described previously [26]. The depletion of target protein was determined by Western blot analysis.

2.9. Construction and transfection of EB1

EB1 cDNA from Beas-2B cells was amplified by RT-PCR using the primers described above, which were designed to introduce KpnI and XhoI restriction sequences at the 5′ and 3′ ends, respectively, of the amplified fragment. The resulting cDNA was cloned into the corresponding restriction sites of the pcDNA3.1/myc-His A vector (Invitrogen). H460 cells were transfected with control vector or EB1 expression vector using Metafectene reagent (Biontex), following the procedure recommended by the manufacturer. Briefly, the Metafectene-DNA complex was incubated at room temperature for 20 min, diluted with serum-free transfection medium, and added to the cells. After incubation in complete medium for 24 h, transfected cells were treated with radiation and incubated for an additional 48 h.

2.10. Western blot analysis

Western blot analyses were performed as described previously [29], and blots were probed with primary antibodies against EB1, Bcl-2, Bcl-xl, Bax, HSP60, cytochrome c, AIF p53, Iκ-B, α-tubulin (Santa Cruz Biotechnology Inc.); cleaved-PARP (Asp214) and cleaved caspase-3 (Cell Signaling Technology, Beverly, MA, USA);

and β-actin (Sigma). Blots were developed using a peroxidase-conjugated secondary antibody and enhanced chemiluminescence (ECL) system (Amersham Life Sciences, Piscataway, NJ, USA).

2.11. Subcellular fractionation

The subcellular distribution of protein was determined by fractionating cells into cytosolic and mitochondrial fractions, followed by Western blotting. For isolation of the cytosolic fraction, cells were lysed with lysis buffer (20 mM HEPES, pH 7.5, 250 mM sucrose, 10 mM KCl, 2 mM $MgCl_2$, 1 mM EDTA, 1 mM DTT, protease inhibitor cocktail) for 20 min on ice. Samples were homogenized by 70 strokes of a Dounce glass homogenizer with a loose pestle (Wheaton, Millville, NJ, USA). The homogenate was centrifuged at 12,000 rpm for 20 min at 4 °C. Levels of cytochrome *c*, AIF, and tubulin protein were determined by Western blot analysis. For isolation of the mitochondrial fraction, the insoluble pellet remaining after collection of the cytosolic fraction was resuspended in buffer (20 mM Tris–HCl, pH 6.7, 0.15 mM $MgCl_2$, 0.25 mM sucrose, 1 mM DTT, protease inhibitor cocktail). After incubation for 30 min on ice, the pellet was centrifuged at 12,000 rpm for 20 min at 4 °C. Mitochondrial levels of Bax and HSP60 protein were determined by Western blot analysis.

2.12. Statistical analysis

Cell culture experiments were repeated at least three times. Statistical differences between groups were assessed by Students *t*-test, and a p-value < 0.05 was considered significant.

3. Results

3.1. Depletion of EB1 alone suppresses the growth of lung cancer cells

We compared the proliferation rate among NSCLC cells (H460, A549 and H1299) without any treatment. Although the relative cell growth rates were different (H460 > A549 > H1299), 24 h was sufficient for a population doubling after seeding for all tested cell lines (Fig. 1A). An analysis of differential expression between parental H460 and radioresistant H460 cell lines revealed the EB1 gene as a radioresistance target (data not shown). We thus examined the role of EB1, focusing on radiation-related cell death in this study. Interestingly, EB1 transcript (Fig. 1B, top) and protein (Fig. 1B, bottom) levels were lower in H460 cells than in A549 and H1299 cells, suggesting that H460 cells would be the most sensitive to radiation. Consistent with the results of Western blotting of Fig. 1B, immunostaining experiments also revealed that EB1 expression was higher in A549 cells than in H460 cells although EB1 was major distributed in the cytoplasm of both A549 and H460 cells (Fig. 1C). To examine whether EB1 regulates cytotoxicity of NSCLC cells, we used siRNA to knock down endogenous EB1 in A549 and H1299 cells, which express high levels of EB1. Depletion of EB1 alone potently enhanced cytotoxicity in both cell lines in a time-dependent manner (Fig. 1D) and dramatically decreased colony formation (Fig. 1E). In addition, clonogenic survival assays showed that EB1-knockdown cells were more sensitive than control cells to exposure to a single dose of radiation ranging from 0 to 5 Gy (Fig. 1F). Thus, our results suggest that EB1 is associated with the development of radioresistance in lung cancer cells.

3.2. EB1 depletion plus radiation treatment induces p53-independent cytotoxicity of lung cancer cells

As expected, H460 cells were the most sensitive to 10 Gy radiation, whereas both A549 and H1299 cells showed a distinct radioresistance to the same radiation dose (Fig. 2A). To better understand the relationship between EB1 expression and the radioresistance phenotype of lung cancer cells, we analyzed the effects of EB1 loss-of-function in EB1 highly expressing A549 and H1299 cells. FACS analyses showed that treatment with 10 Gy radiation alone induced approximately 17% cell death in p53-wild type A549 cells and transfection of EB1 siRNA alone induced approximately 26% cell death; combined stimulation (radiation-plus EB1-knockdown) induced approximately 42% cell death (Fig. 2B, left). Western blotting showed that radiation treatment and/or EB1 depletion caused a marked decrease in the level of EB1 protein in A549 cells in association with a marked elevation in the levels of cleaved PARP and active caspase 3, two important apoptotic markers (Fig. 2B, right). Consistent with these results, morphological changes characteristic of apoptosis were observed in EB1-knockdown- and radiation-treated A549 cells, but not in control cells (Fig. 2C). Interestingly, radiation treatment did not change EB1 protein levels in p53-null type H1299 cells, but the patterns of cell death were very similar to those of A549 cells under the same experimental conditions, as determined by FACS analysis (Fig. 2D, left) and Western blotting (Fig. 2D, right). Taken together, our data suggest the possibility that EB1 mediates a p53-independent apoptotic signal and cross talks with the radiation pathway in a cell-type dependent manner. We further examined whether the correlation between EB1 level and radiosensitivity is universal in other cancer and normal cell lines. Consistent with the results of A549 and H1299 cells, BEAS-2B normal cells and SiHa cancer cells showed strong correlation between EB1 knockdown and radiosensitivity (Fig. 2E). However, EB1 depletion did not induce cell death in HCT 116 and MCF-7 cancer cells and had no effect on radiation-mediated cell death of these cells (Fig. 2E). Therefore, these data suggest that the contribution of an EB1 molecule to the regulation of radiosensitivity can be cell type specific.

3.3. Depletion of EB1 promotes cell death via ROS-dependent Bax induction

Bax translocation to mitochondria is a key event in the induction of apoptotic cell death in several cell lines [30,31]. Thus, we examined whether depletion of EB1 is associated with ROS-dependent activation of Bax in lung cancer cells. We found that knockdown of EB1 alone or in combination with radiation led to down-regulation of Bcl-2 and up-regulation of Bax levels in whole-cell lysates of both A549 and H1299 cells, but did not modulate Bcl-xl levels (Fig. 3A). It is well known that radiation promotes ROS generation during radiotherapy in the lung [32]. FACS analysis (Fig. 3B, top) and cell staining (Fig. 3B, bottom) revealed that EB1 depletion also induced a notable increase in ROS production in A549 cells. This phenomenon of ROS generation could also be detected in other lung cancer H1299 cells (Supplemental Fig. 1A). Moreover, pretreatment with NAC, a ROS scavenger, completely inhibited the increase in Bax expression induced by radiation stimulation of EB1-knockdown A549 cells, whereas the decreased levels of Bcl-2 were not rescued by ROS inhibition (Fig. 3C). These data suggest that EB1-mediated regulation of Bcl-2 and Bax occur via ROS-independent and -dependent pathways, respectively. We further confirmed Bax modulation by examining subcellular fractions under the same experimental conditions. Western blot analyses revealed that the pattern of Bax protein expression in the mitochondrial fraction was consistent with the results obtained using whole-cell lysates (Fig. 3D). Notably, NAC treatment reduced radiation-induced cell death in EB1-knockdown A549 cells by approximately 50% (Fig. 3E, top) and robustly decreased the two apoptotic markers, cleaved PARP and the active form of caspase 3, without rescuing EB1 protein levels (Fig. 3E, bottom), indicating that ROS regulation is down-stream of EB1 in this signaling pathway. The same effects of NAC treatment on cell death were also observed in EB1-knockdown H1299 cells (Supplemental Fig. 1B).

3.4. Bax is a target of the transcription factor NF-κB during EB1-depletion- and radiation-mediated cell death

To examine whether Bax accumulation induced by knockdown of EB1 is associated with NF-κB activation, we investigated

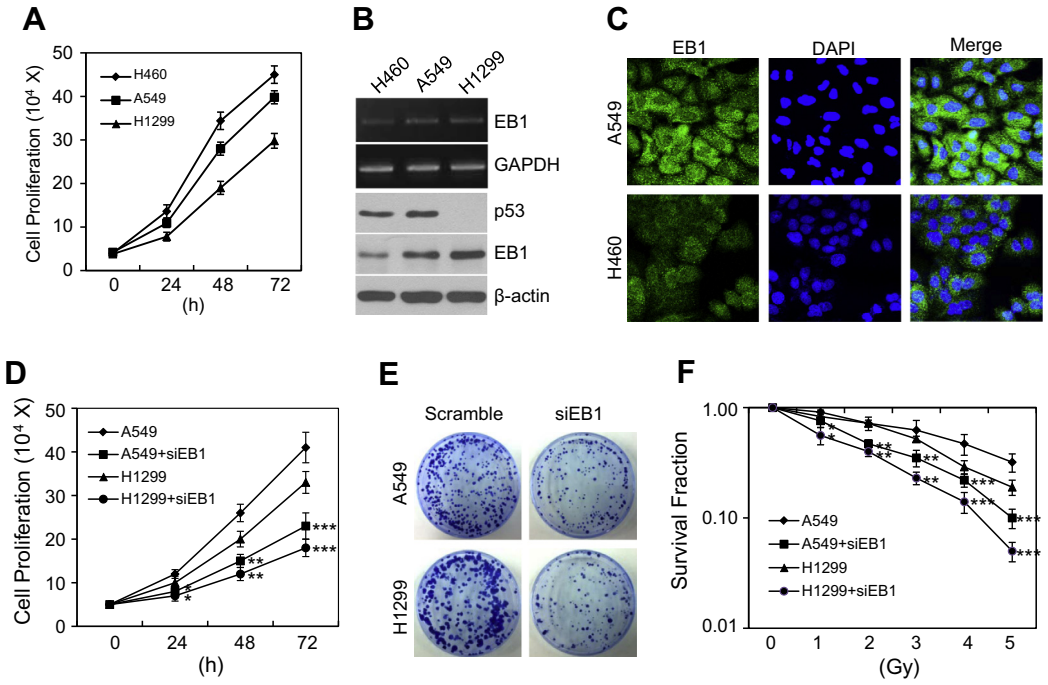

Fig. 1. Effects of EB1 on NSCLC cell proliferation. (A) Proliferation of H460, A549, and H1299 cells after incubating for 24, 48, and 72 h without any treatment. Bars represent standard deviations (SD) of three independent experiments performed in triplicate. (B) EB1 expression in H460, A549, and H1299 cells. *Top:* RT-PCR. *Bottom:* Western blot analysis. GAPDH and β-actin were used as loading controls. (C) Representative confocal images of EB1 localization in A549 and H460 cells. Magnification, 400×. (D) Proliferation of A549 and H1299 cells transfected with 100 nM scrambled (control) or EB1 siRNA and incubated for 24, 48, and 72 h. Data are expressed as means ± SD ($^{*}p < 0.05$, $^{**}p < 0.005$ and $^{***}p < 0.0005$ compared with scrambled siRNA-transfected control cells). (E) Representative image of colony formation by A549 and H1299 cells transfected with 100 nM scrambled or EB1 siRNA 14 days after transfection, visualized with trypan blue staining. (F) Survival fraction of A549 and H1299 cells treated with a single dose of radiation (0–5 Gy) after transfection with 100 nM scrambled or EB1 siRNA, measured 14 days after radiation treatment. Data are expressed as means ± SD ($^{*}p < 0.05$, $^{**}p < 0.005$ and $^{***}p < 0.0005$ compared with scrambled siRNA-transfected control cells).

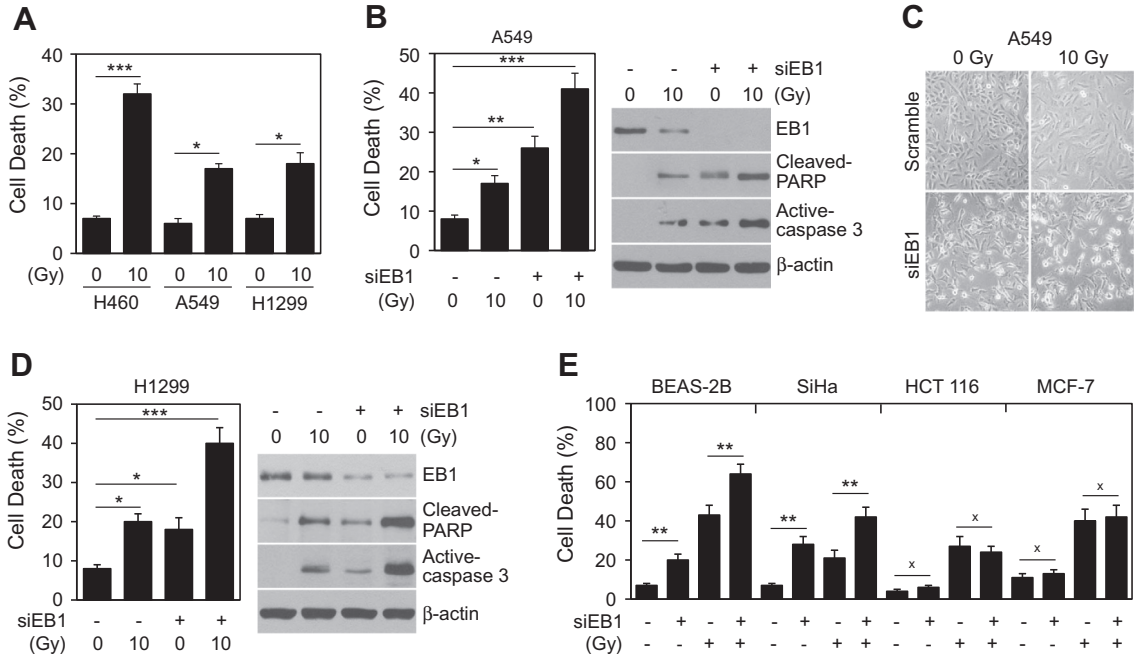

Fig. 2. Effects of EB1 depletion on cell death of radiation-treated NSCLC cells. (A) Analysis of cell death in H460, A549, and H1299 cells, untreated or treated with 10 Gy radiation and then incubated for 48 h. Data are expressed as means ± SD ($^{*}p < 0.05$ and $^{***}p < 0.0001$ compared with untreated controls). (B) Analysis of cell death in A549 cells, untreated or treated with 10 Gy radiation after transfection with 100 nM scrambled or EB1 siRNA and then incubated for 48 h. *Left:* FACS analysis. *Right:* Western blot analysis of cell-death indicators. Data are expressed as means ± SD ($^{*}p < 0.05$, $^{**}p < 0.005$ and $^{***}p < 0.0001$ compared with unstimulated controls). β-actin was used as a loading control. (C) Morphological changes in A549 cells treated as in B (magnification, 100×). (D) Analysis of cell death in H1299 cells treated as in B. *Left:* FACS analysis. *Right:* Western blot analysis of cell-death indicators. Data are expressed as means ± SD ($^{*}p < 0.05$ and $^{***}p < 0.0001$ compared with unstimulated controls). (E) Analysis of cell death in BEAS-2B, SiHa, HCT 116, and MCF-7 cell lines treated as in B. Data of FACS analysis are expressed as means ± SD ($^{**}p < 0.05$ compared with controls).

degradation of IκB, an NF-κB inhibitory protein. EB1 depletion alone or in combination with radiation led to significant down-regulation of IκB protein in A549 cells (Fig. 4A, top). This effect was completely prevented by scavenging ROS with NAC (Fig. 4A, bottom), indicating that increased transcriptional activity of NF-κB is down-stream of ROS signaling. In addition, direct inhibition of IκB phosphorylation with BAY 11-7082 (BAY) clearly enhanced the up-regulation of IκB and subsequent decrease in Bax expression induced by combined stimulation in A549 cells (Fig. 4B). Bcl-2 levels were not altered by treatment with BAY, suggesting that the Bcl-2-dependent mechanism of EB1-mediated A549 cell death is NF-κB-independent (Fig. 4B). We further confirmed Bax modulation by examining mitochondrial fractions under the same experimental conditions, finding a Bax expression pattern that was similar to that obtained with whole-cell lysates (Fig. 4C). Since ROS induced NF-κB activation as above, we examined whether NF-κB signaling maintains a positive feedback loop to induce ROS production. Consistent with the results shown in Fig. 3B, FACS analyses (Fig. 4D, left) and cell staining (Fig. 4D, right) showed that EB1 depletion and/or radiation treatment induced ROS production, but these actions were not blocked by BAY treatment in both A549 and H1299 cells, indicating that NF-kB activation is down-stream of ROS signaling pathway. However, BAY treatment did reduce the cell death induced by combined stimulation in A549 cells by approximately 48% (Fig. 4E, left). Consistent with the results of FACS analyses, Western blotting showed that BAY treatment significantly decreased the levels of cleaved PARP and the active form of caspase 3 in A549 cells without altering EB1 levels (Fig. 4E, right). Taken together, our data suggest that induction of the NF-κB target Bax is a key event in EB1-depletion-mediated cell death.

3.5. Ectopic overexpression of EB1 blocks radiation-induced cell death in H460 cells

To further elucidate the role of EB1 in lung cancer cell death, we examined the effects of EB1 gain-of-function by ectopically over-expressing EB1 in H460 cells, which express low levels of EB1. Although ectopic overexpression of wild-type EB1 alone did not affect the viability of H460 cells compared to control, it reduced the radiation-induced death of these cells by approximately 45% (Fig. 5A, top). Consistent with this pattern of cell death, Western blotting showed that radiation treatment significantly decreased EB1 levels and increased the levels of cleaved PARP and the active form of caspase 3 in parental H460 cells (Fig. 5A, bottom). Notably, the increases in these two apoptotic markers induced by irradiation (10 Gy) of H460 cells were markedly reduced by overexpression of EB1 (Fig. 5A, bottom). Collectively, these data suggest that EB1 might be a biomarker of the radioresistance phenotype in lung cancer cells. We continued our analysis by examining whether EB1 regulates ROS and Bax signaling in H460 cells. In contrast to EB1 knockdown, ectopic EB1 overexpression inhibited radiation-induced ROS production in H460 cells, as determined by FACS analysis (Fig. 5B, top) and cell staining (Fig. 5B, bottom). It also led to an induction of Bcl-2 in parental H460 cells, an effect that was diminished in radiation-treated H460 cells (Fig. 5C, top). Although Bcl-xl levels were unchanged by radiation treatment and/or EB1 accumulation, EB1 overexpression caused a ROS-dependent reduction in the radiation-induced increase in Bax levels in H460 cells (Fig. 5C, top). The pattern of Bax alterations obtained in experiments using the mitochondrial fraction was consistent with these results (Fig. 5C, bottom). Moreover, overexpression of EB1 rescued the radiation-induced down-regulation of IκB levels in H460 cells, indicating that suppression of NF-κB activity is involved in inhibiting Bax expression (Fig. 5D).

3.6. EB1 regulates cell death via p53-independent ROS generation and mitochondrial dysfunction

Recent studies have revealed that ROS act as both an up-stream signal and a down-stream target of p53 [33,34]. We therefore further investigated the relationship between EB1 and p53 expression. siRNA-mediated down-regulation of endogenous EB1 did

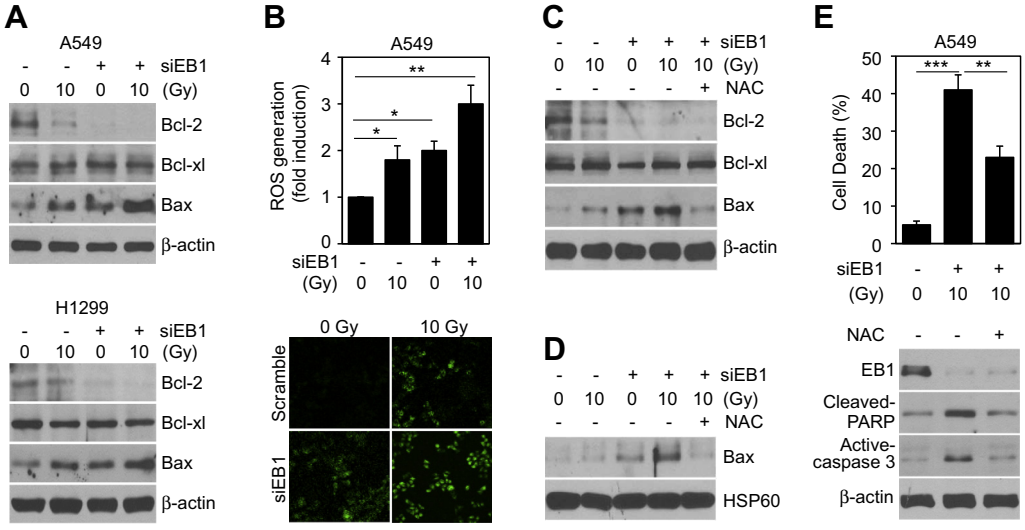

Fig. 3. Effects of EB1 on the expression of Bcl-2 family proteins and ROS generation. (A) Western blot analysis of Bcl-2 family proteins mediating EB1-dependent change in cell death of A549 and H1299 cells, untreated or treated with 10 Gy radiation after transfection with 100 nM scrambled or EB1 siRNA and then incubated for 48 h. β-actin was used as a loading control. (B) ROS generation in A549 cells treated as in A. *Top:* FACS analysis using 10 nM DCF-DA. Bottom: cell staining analyzed by a laser-scanning confocal microscopy (magnification, 100×). Data are expressed as means ± SD (*$p < 0.05$ and **$p < 0.005$ compared with unstimulated controls). (C and D) Western blot analysis of Bcl-2 family proteins in A549 cells treated as in A in the absence or presence of 1 mM NAC. Immunoblot analyses were carried out with whole-cell lysates (C) and mitochondrial fractions (D) using HSP60 as a loading control. (E) Apoptosis analysis in A549 cells treated as in C. *Top:* FACS analysis. *Bottom:* Western blot analysis of cell-death markers. Data are expressed as means ± SD (***$p < 0.0001$ compared with unstimulated controls; **$p < 0.005$ compared with radiation-treated EB1-knockdown cells).

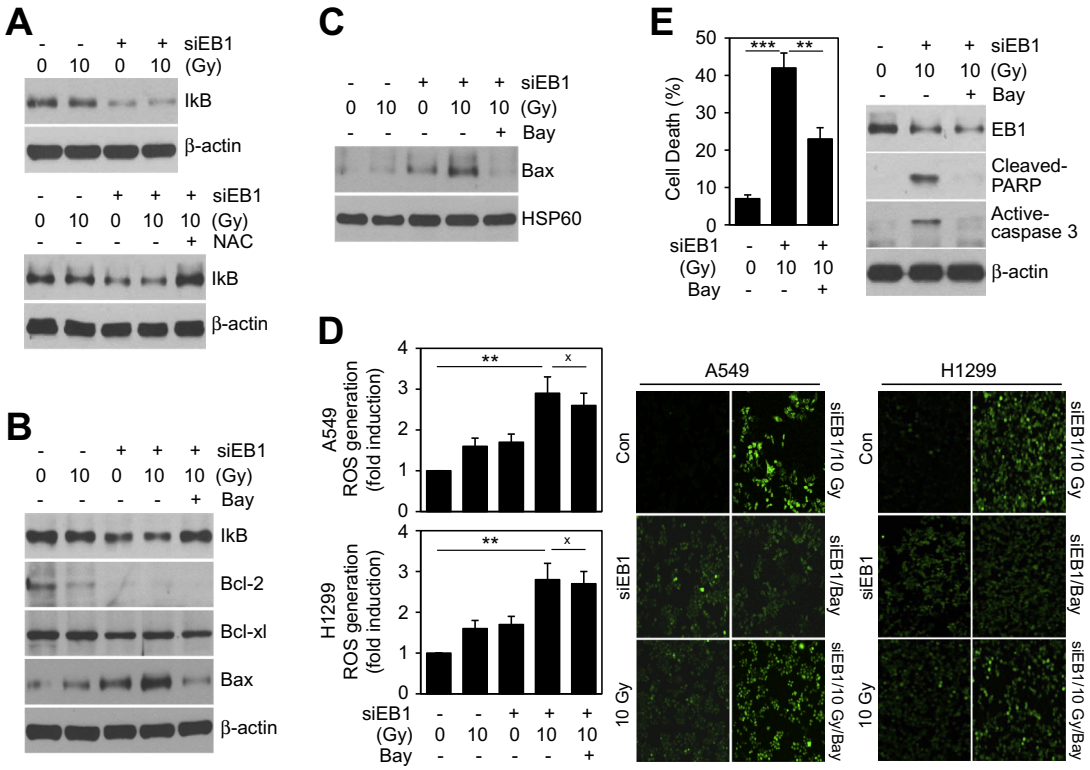

Fig. 4. Effects of NF-κB signaling on Bcl-2 family proteins and apoptosis. (A) Western blot analysis of the NF-κB inhibitor IκB in A549 cells, untreated or treated with 10 Gy radiation after transfection with 100 nM scrambled or EB1 siRNA and incubated for 48 h (top) in the absence or presence of 1 mM NAC (bottom). β-actin was used as a loading control. (B and C) Western blot analysis of IκB and Bcl-2 family proteins in A549 cells, untreated or treated with 10 Gy radiation after transfection with 100 nM scrambled or EB1 siRNA and incubated for 48 h in the absence or presence of 1 μM BAY. Immunoblot analyses were carried out with whole-cell lysates (B) and mitochondrial fractions (C) using HSP60 as a loading control. (D) ROS generation in A549 and H1299 cells treated as in B. Left: FACS analysis with 10 nM DCF-DA. Right: cell staining analyzed by a laser-scanning confocal microscopy (magnification, 100×). Data are expressed as means ± SD (**$p < 0.005$ compared with unstimulated controls; × denotes no significance compared with radiation-stimulated EB1-knockdown cells). (E) Apoptosis analysis in A549 cells treated as in B. *Left:* FACS analysis. *Right:* Western blot analysis of cell-death markers. Data are expressed as means ± SD (***$p < 0.0001$ compared with unstimulated controls; **$p < 0.005$ compared with radiation-stimulated EB1-knockdown cells).

not alter the expression level of p53 in H460, A549 or H1299 cells, although it effectively knocked down EB1 in all cancer cells tested (Fig. 6A). Moreover, ectopic overexpression of p53 had no effect on EB1 levels in p53-null type H1299 cells (Fig. 6B). We further analyzed this relationship using HCT116 $p53^{+/+}$ and $p53^{-/-}$ cancer cell lines treated with 10 Gy radiation. Although radiation induced a time-dependent increase in the level of p53 protein in HCT116 $p53^{+/+}$ cells, EB1 levels were unchanged in both cell lines (Fig. 6C). In an attempt to elucidate the role of EB1 in Bax-mediated mitochondrial dysfunction, we determined the levels of cytochrome c and AIF in cytosolic fraction. EB1 depletion alone or in combination with radiation treatment induced a significant release of cytochrome c and AIF from mitochondria into the cytoplasm in A549 cells, a phenomenon that was completely blocked by BAY treatment (Fig. 6D). In addition, staining of A549 cells with MitoSOX Red to detect mitochondrial ROS after EB1 depeltion and/or radiation treatment in the presence or absence of BAY showed that all stimulation paradigms markedly induced mitochondrial ROS in both A549 and H1299 cells, but NF-κB inhibition with BAY did not diminish these elevated ROS levels (Fig. 6E). Moreover, overexpression of EB1 in H460 cells blocked the radiation-induced release of cytochrome c and AIF (Fig. 6E) and the production of mitochondrial ROS (Fig. 6F). Taken together, these data suggest that knockdown of EB1 acts through ROS production and Bax redistribution to induce mitochondria-mediated cell death.

4. Discussion

The EB1 protein, which is highly conserved from yeasts to humans, localizes to the growing tips of the microtubule plus end. Therefore, the physiological roles of this protein in microtubule dynamics, cell polarity, and genome stability have been largely reviewed [35,36]. However, the molecular pathways by which EB1 controls tumorigenesis and tumor cell growth are only now starting to emerge. We previously identified EB1 as radioresistance- related-gene in laryngeal cancer cells using a proteomic analysis, but the mechanism and extent of these functions are not investigated [26]. Here, we characterized the role and molecular mechanism of EB1 in regulating apoptosis of NSCLC cells in response to radiation through EB1 loss-of-function and gain-of-function strategies.

Scolz et al. [37] suggested that, among its other biological roles, EB1 is necessary for the increased invasive capacity of breast cancer cells through its induction of GTSE1 (G-2 and S-phase expressed 1) activation. Although the cell line used in this previous study was different from those used here, this positive regulatory role of EB1 in promoting tumor cell invasion and metastasis is thoroughly consistent with our demonstration that EB1 inhibits radiation-induced NSCLC cell death. Previous reports also suggested that EB1 is overexpressed in several cancer cell lines and thus might act as an oncogene [21–24]. These studies demonstrated that EB1 functions are primarily attributable to complex formation with APC and subsequently induction of the nuclear

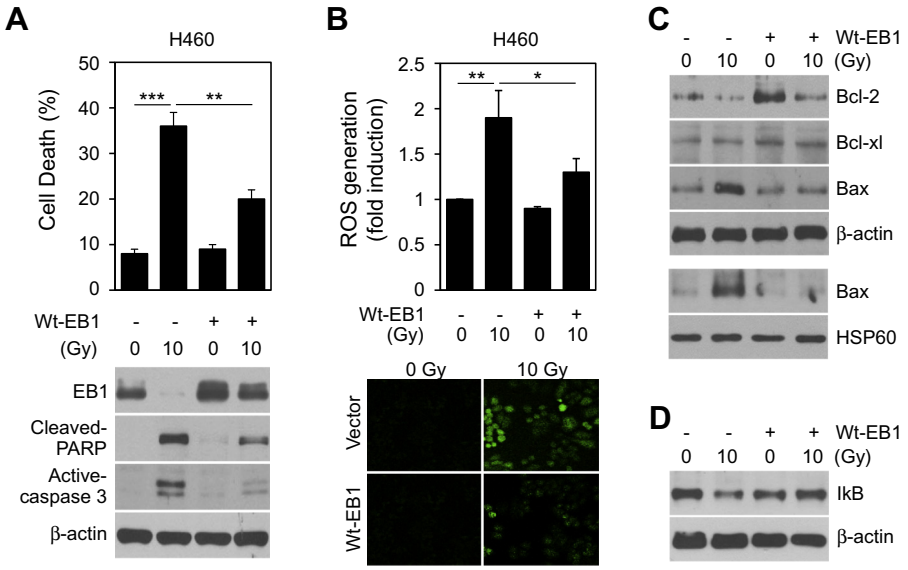

Fig. 5. Effect of EB1 ectopic overexpression on apoptosis in radiation-treated H460 cells. (A) Apoptosis analysis in H460 cells, untreated or treated with 10 Gy radiation after transfection with 3 μg of control vector or EB1 expression vector and then incubated for 48 h. *Top:* FACS analysis. *Bottom:* Western blot analysis of cell death indicators. Data are expressed as means ± SD (***$p < 0.0001$ compared with untreated controls; **$p < 0.005$ compared with radiation treatment). β-actin was used as a loading control. (B) ROS generation in H460 cells treated as in A. Top: FACS analysis with 10 nM DCF-DA. Bottom: Cell staining analyzed by a laser-scanning confocal microscopy (magnification, 100×). Data are expressed as means ± SD (**$p < 0.005$ compared with untreated controls; *$p < 0.05$ compared with radiation treatment). (C) Western blot analysis of Bcl-2 family proteins in H460 cells treated as in A. *Top:* whole-cell lysates. *Bottom:* mitochondrial fraction. HSP60 was used as a loading control. (D) Western blot analysis of IκB in H460 cells treated as in A.

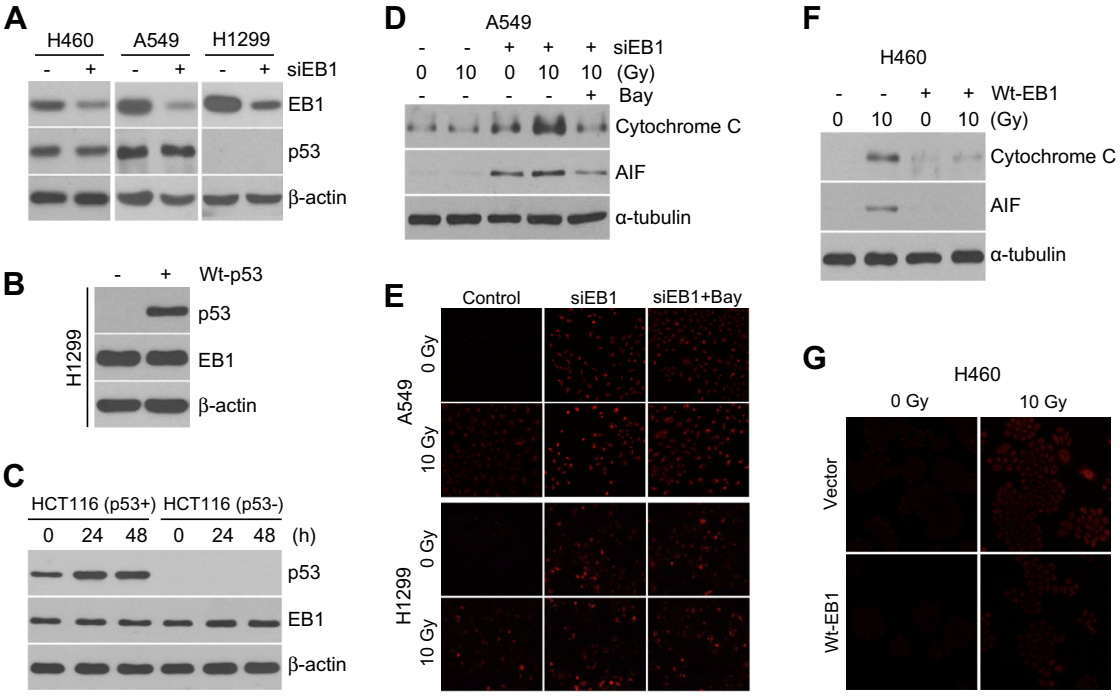

Fig. 6. Effects of EB1 on p53 and mitochondrial function in NSCLC cells. (A) Western blot analysis of p53 in H460, A549, and H1299 cells transfected with 100 nM scrambled or EB1 siRNA and then incubated for 48 h. β-actin was used as a loading control. (B) Western blot analysis of EB1 in H1299 cells transfected with 3 μg of control vector or p53 expression vector and then incubated for 48 h. (C) Western blot analysis of p53 and EB1 in HCT116 $p53^{+/+}$ and HCT116 $p53^{-/-}$ cells treated with 10 Gy radiation for 0, 24, and 48 h. (D) Western blot analysis of cytochrome c and AIF in A549 cells, untreated or treated with 10 Gy radiation after transfection with 100 nM scrambled or EB1 siRNA and then incubated for 48 h in the absence or presence of 1 μM BAY. Immunoblot analyses were carried out with the cytosolic fraction using tubulin as a loading control. (E) Mitochondrial ROS generation in A549 and H1299 cells treated as in D, shown by cell staining with the mitochondrial superoxide indicator MitoSox Red. (F) Western blot analysis of cytochrome c and AIF in H460 cells, untreated or treated with 10 Gy radiation after transfection with 3 μg of control vector or EB1 expression vector and then incubated for 48 h. Immunoblot analyses were carried out using the cytosolic fraction. (G) Mitochondrial ROS generation in H460 cells treated as in F, shown by cell staining with mitochondrial superoxide indicator MitoSox Red.

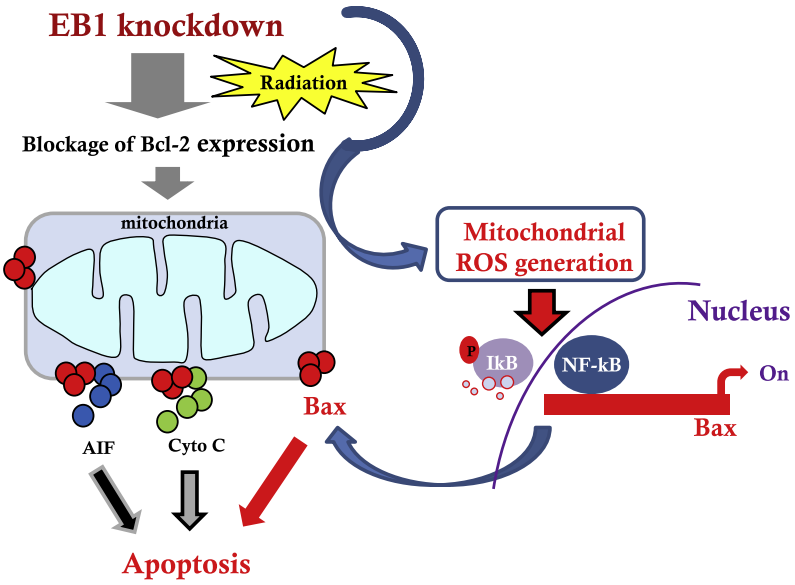

Fig. 7. Schematic summary of the signaling pathway underlying the apoptotic death of NSCLC cells induced by knockdown of EB1 and radiation treatment, alone and in combination.

accumulation of β-catenin through inhibition of direct interactions between APC and β-catenin. The resulting increase in β-catenin enhances the transcriptional activity of T-cell factor/lymphoid enhancing factor (Tcf/Lef). It is well established that the Wnt/β-catenin pathway regulates tumorigenesis and the malignant phenotype of cancer cells by promoting the β-catenin-mediated expression of Tcf/Lef target genes, such as cyclin D1 and c-Myc [38–40]. Therefore, the effects of EB1 on β-catenin dynamics support the possibility that EB1 is an oncogene, although the signaling mechanisms associated with the regulation of cell growth and tumor-development remain to be elucidated. Moreover, information about EB1 pathways that lead to resistance against radiation or anti-cancer drugs is not yet available.

In this study, we added a new signaling pathway to the list of EB1-regulated pathways, showing that EB1 regulates the apoptotic cell death of NSCLC cells. As shown in Fig. 7, knockdown of EB1 expression promoted a remarkable increase in programmed cell death and conversely, elevation of EB1 expression inhibited cell death induced by radiation treatment. Notably, this apoptosis was associated with a decrease in the expression of anti-apoptotic Bcl-2 proteins and an increase in pro-apoptotic Bax. Recent report has been showed that EB1 caused upregulation of the transcriptional activity of c-Myc in 293 cells, and knockdown of c-Myc abrogated induction of EB1-dependent Bcl-2 expression [25]. In addition, activation of NF-κB by hypoxia promoted aortic endothelial cell death via the suppression of Bcl-2 [41]. In similar with above results, our data showed that EB1 depletion with siRNA decreased in protein level of c-Myc (data not shown) and increased in NF-kB activation (Fig. 4A) in A549 cells. Thus, both β-catenin and NF-κB pathways altered by EB1 may be involved in the regulation of Bcl-2 expression. Bcl-2 family members are known to play prominent roles in controlling mitochondrial permeability and altering cytochrome c release following the initiation of cell-death signaling [6,7]. Therefore, our data define a direct role for EB1 in mitochondrial outer membrane permeabilization. Consistent with the potential function of EB1 as a modulator of Bcl-2 family proteins, we demonstrated that EB1 directly inhibited apoptosis of NSCLC cells by blocking mitochondrial dysfunction, thereby enabling cells to acquire a radiation-resistant phenotype. We further showed that depletion of EB1 induced mitochondrial ROS generation, confirming the functional relationship between EB1 and mitochondria. Moreover, ROS-dependent NF-κB activation positively regulated the release of cytochrome c and AIF from mitochondria to the cytosol by promoting Bax translocation from the cytosol to mitochondria. Given that cytochrome c mainly mediates caspase-dependent apoptotic pathway by activating caspase-3 [42] and AIF mediates caspase-independent apoptotic pathways [43], our results suggest that both caspase-dependent and -independent pathways are involved in the EB1-depletion-induced apoptosis of NSCLC cells. Generally, downstream cascades of EB1 signaling in this paper are consistent with a role for apoptotic proteins in the mitochondrial apoptosis pathway identified by previous reports [8–10]. For example, effects of ROS on cell metabolism are well documented in a variety of species. ROS actively contributes to cell-death signaling pathways by damaging nucleic acids, proteins, and lipids in both mitochondria and the cytosol [44]. Thus, we suggest that NSCLC cells with higher mitochondrial ROS production might be those in which EB1 mediates earlier cell death.

The development of chemo- and/or radio-resistance in tumor cells is a major obstacle in the treatment of advanced lung cancer. Since this phenomenon is also associated with recurrence and metastasis, potential tumor-resistance markers have been investigated as prognostic and therapeutic indicators for chemotherapy or radiotherapy. In addition, molecular-targeted therapy could be an alternative to chemotherapy or radiotherapy in the treatment of cancer. For example, gefitinib, a tyrosine kinase inhibitor of epidermal growth factor receptor, exhibits antitumor activity in advanced NSCLC [45]. In the current study, we found that the radiation-induced decrease in EB1 expression accelerated apoptosis of both $p53^{+/+}$ (A549 and H460) and p53-null type (H1299) lung cancer cells, indicating that the contribution of EB1 to the apoptotic response occurred via a p53-independent cell-death signaling pathway. Furthermore, EB1 signaling tightly regulated the expression of Bcl-2 family proteins during the process of apoptotic cell death. Anti-apoptotic proteins, such as Bcl-2 and Bcl-xL, and pro-

apoptotic proteins, such as Bax and Bak, play important roles in regulating the radioresistance phenotype of cancer cells. Thus, in addition to advancing our understanding of the working mechanisms of EB1, the results presented here strongly suggest the future therapeutic potential of this protein in NSCLC.

5. Conflicts of Interest

No potential conflicts of interest were disclosed.

Acknowledgements

This work was supported by the Nuclear Research & Development Program of the National Research Foundation Grant funded by the Korean government (Ministry of Science, ICT and Future Planning).

Appendix A. Supplementary material

Supplementary data associated with this article can be found, in the online version, at http://dx.doi.org/10.1016/j.canlet.2013.07.027.

References

[1] K.M. Ahmed, J.J. Li, NF-kappa B-mediated adaptive resistance to ionizing radiation, Free Radic. Biol. Med. 44 (2008) 1–13.
[2] H.S. Hsu, P.I. Huang, Y.L. Chang, C. Tzao, Y.W. Chen, H.C. Shih, S.C. Hung, Y.C. Chen, L.M. Tseng, S.H. Chiou, Cucurbitacin I inhibits tumorigenic ability and enhances radiochemosensitivity in nonsmall cell lung cancer-derived CD133-positive cells, Cancer 117 (2011) 2970–2985.
[3] M. Krause, K. Gurtner, Y. Deuse, M. Baumann, Heterogeneity of tumour response to combined radiotherapy and EGFR inhibitors: differences between antibodies and TK inhibitors, Int. J. Radiat. Biol. 85 (2009) 943–954.
[4] P. Saintigny, J.A. Burger, Recent advances in non-small cell lung cancer biology and clinical management, Discov. Med. 13 (2012) 287–297.
[5] H.M. McBride, M. Neuspiel, S. Wasiak, Mitochondria: more than just a powerhouse, Curr. Biol. 16 (2006) R551–560.
[6] T. Efferth, M. Giaisi, A. Merling, P.H. Krammer, M. Li-Weber, Artesunate induces ROS mediated apoptosis in doxorubicin-resistant T leukemia cells, PLoS One 2 (2007) e693.
[7] A. Hamacher-Brady, H.A. Stein, S. Turschner, I. Toegel, R. Mora, N. Jennewein, T. Efferth, R. Eils, N.R. Brady, Artesunate activates mitochondrial apoptosis in breast cancer cells via iron-catalyzed lysosomal reactive oxygen species production, J. Biol. Chem. 286 (2011) 6587–6601.
[8] G. Kroemer, J.C. Reed, Mitochondrial control of cell death, Nat. Med. 6 (2000) 513–519.
[9] L. Scorrano, S.J. Korsmeyer, Mechanisms of cytochrome c release by proapoptotic BCL-2 family members, Biochem. Biophys. Res. Commun. 304 (2003) 437–444.
[10] J. Li, Z. Xu, M. Tan, W. Su, X.G. Gong, 3-(4-(Benzo[d]thiazol-2-yl)-1-phenyl-1Hpyrazol-3-yl) phenyl acetate induced HepG2 cell apoptosis through a ROS-mediated pathway, Chem. Biol. Interact. 183 (2010) 341–348.
[11] D.R. Green, G. Kroemer, The pathophysiology of mitochondrial cell death, Science 305 (2004) 626–629.
[12] A. Antignani, R.J. Youle, How do Bax and Bak lead to permeabilization of the outer mitochondrial membrane?, Curr Opin. Cell Biol. 18 (2006) 685–689.
[13] L.K. Su, M. Burrell, D.E. Hill, J. Gyuris, R. Brent, R. Wiltshire, J. Trent, B. Vogelstein, K.W. Kinzler, APC binds to the novel protein EB1, Cancer Res. 55 (1995) 2972–2977.
[14] J.S. Tirnauer, S. Grego, E.D. Salmon, T.J. Mitchison, EB1-microtubule interactions in Xenopus egg extracts: role of EB1 in microtubule stabilization and mechanisms of targeting to microtubules, Mol. Biol. Cell 13 (2002) 3614–3626.
[15] R.A. Green, R. Wollman, K.B. Kaplan, APC and EB1 function together in mitosis to regulate spindle dynamics and chromosome alignment, Mol. Biol. Cell 16 (2005) 4609–4622.
[16] G. Carranza, R. Castaño, M.L. Fanarraga, J.C. Villegas, J. Gonçalves, H. Soares, J. Avila, M. Marenchino, R. Campos-Olivas, G. Montoya, J.C. Zabala, Autoinhibition of TBCB regulates EB1-mediated microtubule dynamics, Cell Mol. Life Sci. 70 (2013) 357–371.
[17] Y. Wen, C.H. Eng, J. Schmoranzer, N. Cabrera-Poch, E.J. Morris, M. Chen, B.J. Wallar, A.S. Alberts, G.G. Gundersen, EB1 and APC bind to mDia to stabilize microtubules downstream of Rho and promote cell migration, Nat. Cell Biol. 6 (2004) 820–830.
[18] J.M. Schober, J.M. Cain, Y.A. Komarova, G.G. Borisy, Migration and actin protrusion in melanoma cells are regulated by EB1 protein, Cancer Lett. 284 (2009) 30–36.
[19] P. Xia, Z. Wang, X. Liu, B. Wu, J. Wang, T. Ward, L. Zhang, X. Ding, G. Gibbons, Y. Shi, X. Yao, EB1 acetylation by P300/CBP-associated factor (PCAF) ensures accurate kinetochore–microtubule interactions in mitosis, Proc. Natl. Acad. Sci. USA 109 (2012) 16564–16569.
[20] F. Jaulin, G. Kreitzer, KIF17 stabilizes microtubules and contributes to epithelial morphogenesis by acting at MT plus ends with EB1 and APC, J. Cell Biol. 190 (2010) 443–460.
[21] W. El-Rifai, H.F. Frierson Jr, J.C. Harper, S.M. Powell, S. Knuutila, Expression profiling of gastric adenocarcinoma using cDNA array, Int. J. Cancer 92 (2001) 832–838.
[22] K. Fujii, T. Kondo, H. Yokoo, T. Yamada, K. Iwatsuki, S. Hirohashi, Proteomic study of human hepatocellular carcinoma using two-dimensional difference gel electrophoresis with saturation cysteine dye, Proteomics 5 (2005) 1411–1422.
[23] Y. Wang, X. Zhou, H. Zhu, S. Liu, C. Zhou, G. Zhang, L. Xue, N. Lu, L. Quan, J. Bai, Q. Zhan, N. Xu, Overexpression of EB1 in human esophageal squamous cell carcinoma (ESCC) may promote cellular growth by activating beta-catenin/TCF pathway, Oncogene 24 (2005) 6637–6645.
[24] X. Dong, F. Liu, L. Sun, M. Liu, D. Li, D. Su, Z. Zhu, J.T. Dong, L. Fu, J. Zhou, Oncogenic function of microtubule end-binding protein 1 in breast cancer, J. Pathol. 220 (2010) 361–369.
[25] M. Liu, S. Yang, Y. Wang, H. Zhu, S. Yan, W. Zhang, L. Quan, J. Bai, N. Xu, EB1 acts as an oncogene via activating beta-catenin/TCF pathway to promote cellular growth and inhibit apoptosis, Mol. Carcinogen. 48 (2009) 212–219.
[26] J.S. Kim, J.W. Chang, H.S. Yun, K.M. Yang, E.H. Hong, D.H. Kim, H.D. Um, K.H. Lee, S.J. Lee, S.G. Hwang, Chloride intracellular channel 1 identified using proteomic analysis plays an important role in the radiosensitivity of HEp-2 cells via reactive oxygen species production, Proteomics 10 (2010) 2589–2604.
[27] E.H. Hong, H.S. Yun, J. Kim, H.D. Um, K.H. Lee, C.M. Kang, S.J. Lee, J.S. Chun, S.G. Hwang, Nicotinamide phosphoribosyltransferase is essential for interleukin-1beta-mediated dedifferentiation of articular chondrocytes via SIRT1 and extracellular signal-regulated kinase (ERK) complex signaling, J. Biol. Chem. 286 (2011) 28619–28631.
[28] E.H. Hong, S.J. Lee, J.S. Kim, K.H. Lee, H.D. Um, J.H. Kim, S.J. Kim, J.I. Kim, S.G. Hwang, Ionizing radiation induces cellular senescence of articular chondrocytes via negative regulation of SIRT1 by p38 kinase, J. Biol. Chem. 285 (2010) 1283–1295.
[29] S.G. Hwang, S.S. Yu, H. Poo, J.S. Chun, C-Jun/activator protein-1 mediates interleukin-1beta-induced dedifferentiation but not cyclooxygenase-2 expression in articular chondrocytes, J. Biol. Chem. 280 (2005) 29780–29787.
[30] K.G. Wolter, Y.T. Hsu, C.L. Smith, A. Nechushtan, X.G. Xi, R.J. Youle, Movement of Bax from the cytosol to mitochondria during apoptosis, J. Cell Biol. 139 (1997) 1281–1292.
[31] F.H. Sarkar, K.M. Wahidur Rahman, Y. Li, Bax translocation to mitochondria is an important event in inducing apoptotic cell death by indole-3-carbinol (I3C) treatment of breast cancer cells, J. Nutr. 133 (2003) 2434S–2439S.
[32] T. Beinert, D. Binder, M. Stuschke, R.A. Jörres, C. Oehm, M. Fleischhacker, O. Sezer, H.G. Mergenthaler, T. Werner, K. Possinger, Oxidant-induced lung injury in anticancer therapy, Eur. J. Med. Res. 25 (1999) 43–53.
[33] B. Liu, Y. Chen, D.K. St, Clair, ROS and p53: versatile partnership, Free Radic. Biol. Med. 44 (2008) 1529–1535.
[34] B. Vurusaner, G. Poli, H. Basaga, Tumor suppressor genes and ROS: complex networks of interactions, Free Radic. Biol. Med. 52 (2012) 7–18.
[35] J.S. Tirnauer, B.E. Bierer, EB1 proteins regulate microtubule dynamics, cell polarity, and chromosome stability, J. Cell Biol. 149 (2000) 761–766.
[36] K.C. Slep, Structural and mechanistic insights into microtubule end-binding proteins, Curr. Opin. Cell Biol. 22 (2010) 88–95.
[37] M. Scolz, P.O. Widlund, S. Piazza, D.R. Bublik, S. Reber, L.Y. Peche, Y. Ciani, N. Hubner, M. Isokane, M. Monte, J. Ellenberg, A.A. Hyman, C. Schneider, A.W. Bird, GTSE1 is a microtubule plus-end tracking protein that regulates EB1-dependent cell migration, PLoS One 7 (2012) e51259.
[38] T.C. He, A.B. Sparks, C. Rago, H. Hermeking, L. Zawel, L.T. da Costa, P.J. Morin, B. Vogelstein, K.W. Kinzler, Identification of c-MYC as a target of the APC pathway, Science 281 (1998) 1509–1512.
[39] M. Shtutman, J. Zhurinsky, I. Simcha, C. Albanese, M. D'Amico, R. Pestell, A. Ben-Ze'ev, The cyclin D1 gene is a target of the beta-catenin/LEF-1 pathway, Proc. Natl. Acad. Sci. USA 96 (1999) 5522–5527.
[40] J. Mazieres, B. He, L. You, Z. Xu, D.M. Jablons, Wnt signaling in lung cancer, Cancer Lett. 222 (2005) 1–10.
[41] H. Matsushita, R. Morishita, T. Nata, M. Aoki, H. Nakagami, Y. Taniyama, K. Yamamoto, J. Higaki, K. Yasufumi, T. Ogihara, Hypoxia-induced endothelial apoptosis through nuclear factor-kappaB (NF-kappaB)-mediated bcl-2 suppression: in vivo evidence of the importance of NF-kappaB in endothelial cell regulation, Circ. Res. 86 (2000) 974–981.

[42] A. Autret, S.J. Martin, Emerging role for members of the Bcl-2 family in mitochondrial morphogenesis, Mol. Cell 36 (2009) 355–363.
[43] M.A. Gallego, B. Joseph, T.H. Hemström, S. Tamiji, L. Mortier, G. Kroemer, P. Formstecher, B. Zhivotovsky, P. Marchetti, Apoptosis-inducing factor determines the chemoresistance of non-small-cell lung carcinomas, Oncogene 23 (2004) 6282–6291.
[44] E. Cadenas, K.J.A. Davies, Mitochondrial free radical generation, oxidative stress, and aging, Free Radic. Biol. Med. 29 (2000) 222–230.
[45] R.S. Herbst, Dose-comparative monotherapy trials of ZD1839 in previously treated non-small cell lung cancer patients, Semin. Oncol. 30 (2003) 30–38.